Chinese Journal of Aeronautics, (2018), 31(2): 262–272

Chinese Society of Aeronautics and Astronautics
& Beihang University

Chinese Journal of Aeronautics

cja@buaa.edu.cn
www.sciencedirect.com

Modeling and control for cooperative transport of a slung fluid container using quadrotors

Hassan SAYYAADI *, **Ali SOLTANI**

School of Mechanical Engineering, Sharif University of Technology, Tehran 11155-9567, Iran

Received 23 August 2016; revised 15 February 2017; accepted 14 August 2017
Available online 27 December 2017

KEYWORDS

Cooperative transport;
Dynamic modeling;
Liquid sloshing;
Lyapunov stability;
Pose control;
Quadrotors;
Slung load

Abstract In this paper, dynamic modeling and control problem for transfer of a sloshing liquid container suspended through rigid massless links from a team of quadrotors are investigated. By the proposed solution, pose of the slung container and fluid sloshing modes are stabilized appropriately. Dynamics of the container-liquid-quadrotors system is modeled by Euler-Lagrange method. Fluid slosh dynamics is included using multi-mass-spring model. According to derived model, a proper control law is designed for a system with three or more quadrotors. Implementing the proposed control law, quadrotors can control pose of the container, directions of the links and liquid sloshing modes simultaneously. Stability of closed loop system of tracking errors and sloshing modes are demonstrated using a theory of singularly perturbed systems and Lyapunov stability theorem. Also, the capability of the proposed feedback control laws in solving a formerly organized transport problem of a liquid filled container has been demonstrated in simulations. Moreover, priority of the proposed control scheme to an existing slung load controller in the literature is demonstrated.

1. Introduction

Control of partially filled liquid containers on desired trajectories under effect of liquid sloshing has aroused interest of many researchers. For example in study,[1] a general framework to control space manipulators with complex payloads such as payloads with sloshing fluid has been introduced. In another study,[2] two methods for controlling surface of liquid in an open container carried by a robot arm have been proposed by considering fundamental mode of liquid oscillation. An infinite impulse response filter to alter the acceleration profile and tilting the container parallel to the beginning and ending wave are the implemented methods to control the liquid surface properly, which have been examined experimentally. Furthermore, in another research,[3] a reduced 7th order robust H_∞ controller has been designed to control launch vehicle with sloshing fuel in presence of disturbances, structured and unstructured parameter uncertainties. In order to construct a high speed transfer system for a liquid container that satisfies

* Corresponding author.
E-mail addresses: sayyaadi@sharif.edu (H. SAYYAADI), asoltani@mech.sharif.edu (A. SOLTANI).

Peer review under responsibility of Editorial Committee of CJA.

Production and hosting by Elsevier

https://doi.org/10.1016/j.cja.2017.12.005
1000-9361

the reduction of endpoint residual vibration and has robustness against changes in the static liquid level, a suitable nominal model has been adopted and an appropriate reference trajectory has been determined by the optimization in another research.[4] Based on the command inputs and using the suitable nominal model, an H_∞ feedback control system has been applied to this process, and its effectiveness has been shown through simulations and experiments. Furthermore, an active control method that takes into account the rotational and translational motion of the container has been presented, which can achieve complete suppression of sloshing during the whole transfer process. Moreover, to suppress sloshing in the container during acceleration and deceleration along an inclined transfer path, authors in the study[5] have presented a method to actively control the container's rotational motion. The effectiveness of the proposed method has been demonstrated through simulations and experiments. Also, research[6] presents a trajectory control design method to suppress residual vibration in transfer systems without the need to directly measure vibration which needs a large number of complicated sensors. The proposed method consists of two parts. First part is about shaping frequency characteristics of the controller to suppress the vibration. In the second part, various parameters of the control elements are determined by solving an optimization problem with penalty terms expressed by the constraints of both of the time and frequency domains. The effectiveness of the control design method is shown by experiments. Furthermore, in another study[7] and in a similar work,[8] a method is proposed for the design of a switching surface in presence of mismatched uncertainties. Also, a design method for a sliding mode observer based on high gain is proposed in this paper to reconstruct the states of the system for implementation of the sliding mode control. The proposed method is implemented for slosh-free motion of a container in simulations and experiments. In another research,[9] authors have studied modeling and control problem for planar maneuvering of space vehicles with fuel slosh dynamics. A multi-mass–spring model is considered for characterization of the most prominent sloshing modes. Moreover, a Lyapunov-based nonlinear feedback control law has been designed to achieve the control objective which has been examined in simulations. In another work, the authors have investigated the point-to-point liquid container transfer control problem for a robot with two prismatic and one revolute joints.[10] In continuation of their research,[11] they proposed a solution for thrust vector control problem for an upper-stage rocket with fuel slosh dynamics. In both of these studies,[10,11] performance of the proposed control laws has been examined by simulations. In a recent work,[12] authors have presented two methods to reduce an infinite number of sloshing modes in a moving liquid container. The first method is command smoothing to eliminate slosh by using the first-mode frequency, while the second one is a combined input-shaping and command-smoothing architecture. The input shaper reduces slosh for the first mode and the command smoother suppresses slosh for the third and higher modes. Experiments have validated the simulated dynamic behavior and the effectiveness of the methods.

Unmanned Aerial Vehicles (UAVs) are implemented in various operations such as search and rescue operations, military missions and urban operations.[13] In these missions, it may be necessary that UAVs carry a payload. Load transport may be performed by a single quadrotor[14–31] or by a team of UAVs.[32–37] In some of these studies, load is gripped by UAVs.[28,32,37] However, in most of the studies about load transport by aerial robots, the load is suspended from UAVs.[14–27,29–31,33–36] If the load is cable suspended, the system of equations of motion will be hybrid because the cables can be slack or taut during the motion. Therefore, dynamics of the system will be switching. Hybrid nature of slung load systems has been investigated in some studies.[29,38] Moreover, cable suspended load and UAV system can be considered as an *n*-link robotic manipulator with flexible links. Interesting researches about such robots can be found in the literature.[39–41] In the following, some of the studies about slung load transport by UAVs are described in more detail. For instance, dynamic modeling and control of a helicopter with a slung load has been investigated in work.[23] Authors have modeled behavior of representative trim variable values (i.e. cable angle and longitudinal and lateral cyclic blade pitch angles) and modes (i.e. flight dynamics and load modes) due to changes of some model parameters (e.g. cable length, load mass, and equivalent flat plate area). Moreover, they have designed variance constrained controllers for the system. Most of the works about suspended load control by quadrotors have been reported by GRASP laboratory. For example, in study,[32] control laws for grasping and transporting a payload on three-dimensional trajectories by a team of quadrotors have been presented and tested in experiments appropriately. Also, in another study,[29] trajectory generation and control of a quadrotor with a cable suspended point-mass load especially in planar transports have been studied, and proposed controllers were examined experimentally. In the work,[18] authors have extended their geometric control laws for three-dimensional transport. In a research about aerial transport of slung payloads,[33] feasible trajectories for cooperative transport of cable suspended payloads (rigid bodies or point-masses) from quadrotors have been generated by demonstrating that system is a hybrid differentially flat system. Authors in their another paper[34] have designed a controller for quadrotors to transport a cable suspended mass-point load on a desired trajectory while maintaining a relative formation. Also, a similar research[36] has been reported for rigid body load case when number of quadrotors are more than or equal to six. In a more restricted mission,[35] proper control law has been proposed for trajectory control of a cable suspended rigid body load by a team of quadrotors when number of members is more than or equal to three.

In all of the mentioned aerial transport researches, the payload is considered as a rigid body or mass-point, and its inert properties are assumed to be constant. However, if the payload contains sloshing fluid, this assumption will not be correct and the proposed control laws lose their effectiveness in precise trajectory tracking surely. For instance, by proposing a nonlinear model for dynamic behavior of tank vehicles with sloshing fluid in the study,[42] it has been demonstrated that tank vehicle may be unstable under certain operations and road conditions.

Therefore, modeling and control problem for planar aerial transport missions of a sloshing fluid container suspended from a team of quadrotors via massless links are studied in the present study. In spite of the existing studies in the literature, controllers are designed in the present study, so that quadrotors can stabilize the slung container at a desired pose and suppress sloshing modes of the liquid simultaneously. To consider fluid sloshing in dynamic modeling of the system, sloshing modes are modeled by multi spring-mass systems. The proposed control scheme consists of a load pose and fluid sloshing controller, controllers of the links directions and attitude controllers of the quadrotors. Controller of the load pose and fluid sloshing together with the controller of the links directions determine thrust forces and desired attitudes of the quadrotors. Then, each quadrotor uses its attitude controller to track its desired attitude. This paper is organized as follows:

In dynamic modeling section, equations of motion of the considered system are formulated by Euler-Lagrange method. In the next section, control laws are proposed. Moreover, Lyapunov stability theorem along with a theorem of singularly perturbed systems is implemented to prove stability of the closed loop system of tracking errors in appendices. In simulation section, stabilizing mission of a container suspended from three quadrotors via three massless rigid links is organized to verify performance of the designed controllers. To have more accurate verification, initial conditions and properties of container and fluid are brought from the literature. Furthermore, capabilities of the proposed control law are compared with the existing results in the literature. Finally, summary of the paper is presented briefly.

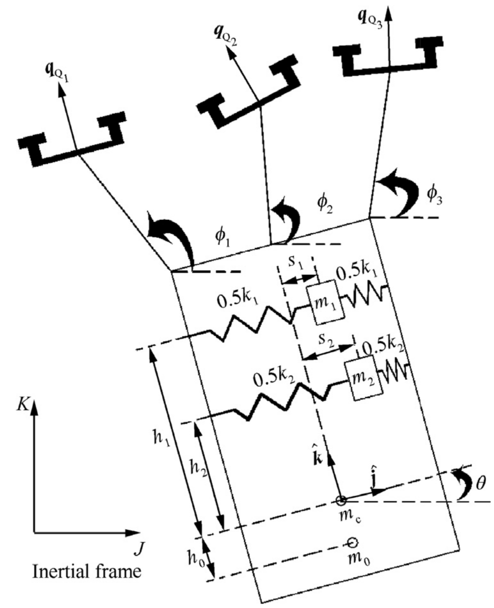

Fig. 1 Multi-mass-spring model of liquid sloshing and container suspended from quadrotors via massless rigid links.

2. Dynamic modeling

This section formulates dynamics of a team of n quadrotors moving a liquid filled container via rigid massless links in a vertical plane including prominent liquid sloshing modes.

Remark 1. Actually, links cannot be completely rigid and massless in practice. However, if mass of the links is small enough, their inertial effects on dynamics of the system can be neglected. Therefore, links are assumed to be massless in many studies such as researches[35,36] similarly. Furthermore, if magnitudes of forces and torques acting on a link are small in comparison with its stiffness, rigidity assumption will be reasonable. This assumption has been made in studies[35,36] too.

Centers of masses of the quadrotors and container and attachment points of the rigid links are supposed to be in the same vertical plane as shown in Fig. 1, θ represents angle between positive directions of y-axes of body fixed and inertial frames, ϕ_i represents angle between ith link and positive direction of y-axis of inertial frame and $\boldsymbol{q}_{Q_i}$ represents unit vector along thrust of ith quadrotor. Therefore, quadrotors should not perform any yaw or pitch motion at all. In other words, yaw and pitch angles of the quadrotors should be controlled at zero. Furthermore, the links have been pivoted to the container and center of mass of the quadrotors. Therefore, links do not affect rotational motion of the quadrotors. Mass and rolling moment of inertia for each quadrotor are denoted by m_{Q_i} and J_{Q_i} respectively while m_c and I_c represent container mass and moment of inertia about x axis of its body fixed frame respectively. In particular, sloshing liquid is modeled as a multi-mass-spring system where oscillation frequencies of mass-spring elements represent m modes of sloshing. Therefore, fluid is modeled by moment of inertia I_0 assigned to a rigidly attached mass m_0 and point masses $m_i, i = 1, 2, \ldots, m$, whose relative positions along container-fixed lateral axis are denoted by s_i. Each sloshing mode is modeled via restoring force $-k_i s_i$ (k_i represents stiffness of ith sloshing mode equivalent spring) which acts on the mass m_i whenever the mass is displaced from its neutral position $s_i = 0$. For simplicity, it is assumed that the center of mass of the container is at the same location as the center of mass of the undisturbed liquid. Vertical locations of liquid masses in the container fixed frame denoted by h_0 and h_i are represented with respect to the center of mass of undisturbed liquid. The parameters $m_0, m_i, I_0, h_0, h_i, k_i$ depend on the shape of the container, the characteristics of the liquid, and the fill ratio of the container.

Moreover, to preserve the static properties of the liquid, the sum of all the masses must be the same as the fluid mass m_f, and the center of mass of the model must be at the same elevation as that of the liquid, i.e.

$$\begin{cases} m_0 + \sum_{i=1}^{m} m_i = m_f \\ m_0 h_0 + \sum_{i=1}^{m} m_i h_i = 0 \end{cases} \tag{1}$$

As demonstrated in Fig. 1, $\hat{\boldsymbol{j}}$ and $\hat{\boldsymbol{k}}$ are transverse and cylindrical axes of the container fixed frame respectively. In the following, position vector of the container center of mass in inertial frame is denoted by $\boldsymbol{r}_c$ while $\boldsymbol{a}_i$ represents position vector of the attachment point of the ith link in the body fixed frame of the container. Moreover, l_i denotes length of the ith link. Furthermore, rotation matrix of inertial frame to the body fixed frame of the container $\boldsymbol{R}_c$ and unit vector along the ith link $\boldsymbol{q}_{p_i}$ are determined by

$$\begin{cases} \boldsymbol{R}_c = \begin{bmatrix} \cos\theta & -\sin\theta \\ \sin\theta & \cos\theta \end{bmatrix} \\ \boldsymbol{q}_{p_i} = \begin{bmatrix} \cos\phi_i \\ \sin\phi_i \end{bmatrix} \end{cases} \tag{2}$$

Definitions of θ and ϕ_i are obvious from Fig. 1. Consequently, position of the masses of the system in inertial frame can be found from the following equations:

$$\begin{cases} \boldsymbol{r}_{Q_i} = \boldsymbol{r}_c + \boldsymbol{R}_c \boldsymbol{a}_i + l_i \boldsymbol{q}_{p_i} & i = 1, 2, \ldots, n \\ \boldsymbol{r}_{m_i} = \boldsymbol{r}_c + s_i \hat{\boldsymbol{j}} + h_i \hat{\boldsymbol{k}} & i = 1, 2, \ldots, m \\ \boldsymbol{r}_{m_0} = \boldsymbol{r}_c + h_0 \hat{\boldsymbol{k}} \end{cases} \tag{3}$$

in which $\boldsymbol{r}_{Q_i}$ represents position vector of ith quadrotor center of mass in inertial frame, $\boldsymbol{r}_{m_i}$ represents position vector of equivalent mass for ith sloshing mode in inertial frame and $\boldsymbol{r}_{m_0}$ represents position vector of static fluid center of mass in inertial frame.

Therefore, kinetic energies of each quadrotor T_{Q_i}, fluid T_f and container T_c can be computed as

$$\begin{cases} T_{Q_i} = \frac{1}{2} m_{Q_i} \dot{\boldsymbol{r}}_{Q_i}^{\mathrm{T}} \dot{\boldsymbol{r}}_{Q_i} + \frac{1}{2} J_{Q_i} \dot{\phi}_{Q_i}^2 \\ T_f = \frac{1}{2} \sum_{i=0}^{m} m_i \dot{\boldsymbol{r}}_{m_i}^{\mathrm{T}} \dot{\boldsymbol{r}}_{m_i} + \frac{1}{2} I_0 \dot{\theta}^2 \\ T_c = \frac{1}{2} m_c \dot{\boldsymbol{r}}_c^{\mathrm{T}} \dot{\boldsymbol{r}}_c + \frac{1}{2} I_c \dot{\theta}^2 \end{cases} \tag{4}$$

in which $\dot{\phi}_{Q_i}$ is rolling angular velocity of the ith quadrotor, $\dot{\boldsymbol{r}}_{Q_i}$ is velocity of ith quadrotor center of mass in inertial frame, $\dot{\boldsymbol{r}}_{m_i}$ is velocity of ith mass of liquid including static and sloshing masses in inertial frame, $\dot{\boldsymbol{r}}_c$ is velocity of container center of mass in inertial frame, $\dot{\theta}$ is angular velocity of container in x-direction. On the other hand, potential energy of the system U can be calculated from

$$U = \sum_{i=1}^{n} m_{Q_i} g z_{Q_i} + (m_f + m_c) g z_c + \frac{1}{2} \sum_{i=1}^{m} k_i s_i^2 \tag{5}$$

in which z_c is z coordinate of container center of mass in inertial frame, z_{Q_i} is z coordinate of ith quadrotor center of mass in inertial frame, g is gravity acceleration.

Now, Lagrangian L_{sys} can be defined as

$$L_{sys} = \sum_{i=1}^{n} T_{Q_i} + T_f + T_c - U \tag{6}$$

It should be noted that a fraction of kinetic energy of sloshing liquid is dissipated during each cycle of the motion. Consequently, dissipative effects due to liquid sloshing are included via a Rayleigh dissipation function given by $R_{\mathrm{damp}} = \frac{1}{2}\sum_{i=1}^{m} c_i \dot{s}_i^2$ in which c_i denotes damping coefficient of each mode, $\dot{s}_i$ is velocity of equivalent mass for ith sloshing mode in body fixed frame. Furthermore, aerodynamic forces acting on container and quadrotors are assumed to be negligible.

As depicted in Fig. 2, thrust forces u_i and rolling torques of quadrotors τ_i^{roll} are inputs of the system.

Applying Lagrange's formulation with dissipation and input forces and torques, equations of motion can be obtained as

$$\begin{cases} \boldsymbol{M}(\boldsymbol{\chi}) \ddot{\boldsymbol{\chi}} + \boldsymbol{f}(\boldsymbol{\chi}, \dot{\boldsymbol{\chi}}) = \boldsymbol{E}(\boldsymbol{\chi}) \boldsymbol{u} \\ \dot{\boldsymbol{q}}_{Q_i} = \dot{\phi}_{Q_i} \times \boldsymbol{q}_{Q_i} \\ J_{Q_i} \ddot{\phi}_{Q_i} = \tau_i^{\mathrm{roll}} \\ \boldsymbol{\chi} = [\boldsymbol{p} \quad \boldsymbol{S} \quad \boldsymbol{\phi}]^{\mathrm{T}} \\ \boldsymbol{p} = [y_c \quad z_c \quad \theta]^{\mathrm{T}} \\ \boldsymbol{S} = [s_1 \quad s_2 \quad \ldots \quad s_m]^{\mathrm{T}} \\ \boldsymbol{\phi} = [\phi_1 \quad \phi_2 \quad \ldots \quad \phi_n]^{\mathrm{T}} \end{cases} \tag{7}$$

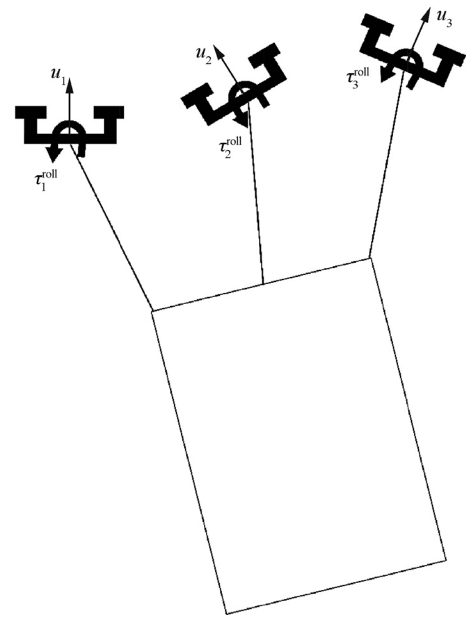

Fig. 2 Thrust forces and rolling torques.

in which $\dot{\boldsymbol{q}}_{Q_i}$ is first derivative of $\boldsymbol{q}_{Q_i}$ with respect to time (velocity of thrust force direction), $\ddot{\phi}_{Q_i}$ is angular acceleration of ith quadrotor in x-direction, y_c is y coordinate of container center of mass in inertial frame.

In Eq. (7), matrix $\boldsymbol{M}(\boldsymbol{\chi})$ can be represented as

$$\boldsymbol{M} = \begin{bmatrix} \boldsymbol{M}_{pp} & \boldsymbol{M}_{ps} & \boldsymbol{M}_{pq} \\ \boldsymbol{M}_{ps}^{\mathrm{T}} & \boldsymbol{M}_{ss} & \boldsymbol{0}_{m \times n} \\ \boldsymbol{M}_{pq}^{\mathrm{T}} & \boldsymbol{0}_{n \times m} & \boldsymbol{M}_{qq} \end{bmatrix} \tag{8}$$

in which matrices $\boldsymbol{M}_{pp}, \boldsymbol{M}_{ps}, \boldsymbol{M}_{pq}, \boldsymbol{M}_{ss}$ and $\boldsymbol{M}_{qq}$ are defined by the following equations:

$$\begin{cases} \boldsymbol{M}_{pp} = \begin{bmatrix} m_t \boldsymbol{I}_{2\times 2} & \boldsymbol{M}_{r\theta} \\ \boldsymbol{M}_{r\theta}^{\mathrm{T}} & m_0 h_0^2 + I_0 + I_c + \sum_{i=1}^{m} m_i (s_i^2 + h_i^2) + \sum_{i=1}^{n} m_{Q_i} \|\boldsymbol{a}_i\|^2 \end{bmatrix} \\ m_t = m_c + m_f + \sum_{i=1}^{n} m_{Q_i} \\ \boldsymbol{M}_{r\theta} = \begin{bmatrix} -\sin\theta \\ \cos\theta \end{bmatrix} \sum_{i=1}^{m} m_i s_i + \boldsymbol{R}_c' \sum_{i=1}^{n} m_{Q_i} \boldsymbol{a}_i \\ \boldsymbol{R}_c' = -\begin{bmatrix} \sin\theta & \cos\theta \\ -\cos\theta & \sin\theta \end{bmatrix} \end{cases} \tag{9}$$

$$\begin{cases} \boldsymbol{M}_{ps} = \begin{bmatrix} \begin{bmatrix} \cos\theta \\ \sin\theta \end{bmatrix} \boldsymbol{m}_s \\ \boldsymbol{D}(\boldsymbol{m}_s) \boldsymbol{h}^{\mathrm{T}} \end{bmatrix} \\ \boldsymbol{m}_s = [m_1 \quad m_2 \quad \ldots \quad m_m] \\ \boldsymbol{h} = [h_1 \quad h_2 \quad \ldots \quad h_m] \end{cases} \tag{10}$$

in which $\boldsymbol{D}(\cdot)$ represents diagonal matrix of a vector.

$$\begin{cases} \boldsymbol{M}_{pq} = \begin{bmatrix} [\, m_{Q_1} l_1 \boldsymbol{q}_{n_1}, \quad m_{Q_2} l_2 \boldsymbol{q}_{n_2}, \quad \ldots, \quad m_{Q_n} l_n \boldsymbol{q}_{n_n} \,] \\ \left[m_{Q_1} l_1 (\boldsymbol{R}_c' \boldsymbol{a}_1)^{\mathrm{T}} \boldsymbol{q}_{n_1}, \quad m_{Q_2} l_2 (\boldsymbol{R}_c' \boldsymbol{a}_2)^{\mathrm{T}} \boldsymbol{q}_{n_2}, \quad \ldots, \quad m_{Q_n} l_n (\boldsymbol{R}_c' \boldsymbol{a}_n)^{\mathrm{T}} \boldsymbol{q}_{n_n} \right] \end{bmatrix} \\ \boldsymbol{q}_{n_i} = \begin{bmatrix} -\sin\phi_i \\ \cos\phi_i \end{bmatrix} \end{cases} \tag{11}$$

$$\boldsymbol{M}_{ss} = \boldsymbol{D}(\boldsymbol{m}_s) \tag{12}$$

$$\begin{cases} \boldsymbol{M}_{qq} = \boldsymbol{D}(m_Q \boldsymbol{l}^2) \\ m_Q \boldsymbol{l}^2 = \begin{bmatrix} m_{Q_1} l_1^2 & m_{Q_2} l_2^2 & \ldots & m_{Q_n} l_n^2 \end{bmatrix} \end{cases} \tag{13}$$

in which $\boldsymbol{l}$ represents vector of lengths of links.

Remark 2. In the recent equations, $\boldsymbol{D}(\boldsymbol{\zeta})$ is a diagonal matrix whose diagonal elements are composed by vector $\boldsymbol{\zeta} = [\,\zeta_1 \quad \zeta_2 \quad \ldots \quad \zeta_n\,]$, ζ_i is damping ratio of ith sloshing mode.

Also, vector $\boldsymbol{f}$ in Eq. (7) can be represented as $\boldsymbol{f} = \begin{bmatrix} \boldsymbol{f}_p \\ \boldsymbol{f}_s \\ \boldsymbol{f}_q \end{bmatrix}$ where

$$\boldsymbol{f}_p = \begin{bmatrix} \boldsymbol{f}_p \\ \boldsymbol{f}_p^\theta \end{bmatrix}$$

$$\begin{aligned} \boldsymbol{f}_p = {} & \left(\boldsymbol{R}_c \sum_{i=1}^{n} m_{Q_i} \boldsymbol{a}_i - \begin{bmatrix} \cos\theta \\ \sin\theta \end{bmatrix} \sum_{i=1}^{m} m_i s_i \right) \dot{\theta}^2 \\ & + m_t \begin{bmatrix} 0 \\ g \end{bmatrix} + 2 \begin{bmatrix} -\sin\theta \\ \cos\theta \end{bmatrix} \dot{\theta} \sum_{i=1}^{m} m_i \dot{s}_i - \sum_{i=1}^{n} m_{Q_i} l_i \boldsymbol{q}_{p_i} \dot{\phi}_i^2 \\ \boldsymbol{f}_p^\theta = {} & [\cos\theta \quad -\sin\theta] \sum_{i=1}^{n} m_{Q_i} \boldsymbol{a}_i g \\ & + \sum_{i=1}^{n} m_{Q_i} l_i (\boldsymbol{R}_c \boldsymbol{a}_i)^{\mathrm{T}} \boldsymbol{q}_{p_i} \dot{\phi}_i^2 + 2\dot{\theta} \sum_{i=1}^{m} m_i \dot{s}_i s_i \end{aligned} \tag{14}$$

in which $\boldsymbol{q}_{p_i}$ is unit vector along i^{th} link.

$$\boldsymbol{f}_s = \boldsymbol{D}(\boldsymbol{c})\dot{\boldsymbol{S}} + (\boldsymbol{D}(\boldsymbol{k}) - \dot{\theta}^2 \boldsymbol{D}(\boldsymbol{m}))\boldsymbol{S} \tag{15}$$

in which $\boldsymbol{c}$, $\boldsymbol{k}$ and $\boldsymbol{m}$ represent vector of damping coefficients of sloshing modes, stiffness of sloshing mode equivalent spring and equivalent mass of sloshing.

$$\boldsymbol{f}_{q_i} = m_{Q_i} l_i (g \cos\phi_i - (\boldsymbol{R}_c \boldsymbol{a}_i)^{\mathrm{T}} \boldsymbol{q}_{p_i} \dot{\theta}^2) \quad i = 1, 2, \ldots, n \tag{16}$$

Moreover, matrix $\boldsymbol{E}$ in equations of motion (7) is determined by

$$\boldsymbol{E} = \begin{bmatrix} \boldsymbol{I}_{2\times2} & \boldsymbol{I}_{2\times2} & \ldots & \boldsymbol{I}_{2\times2} \\ \boldsymbol{R}_c' \boldsymbol{a}_1 & \boldsymbol{R}_c' \boldsymbol{a}_2 & \ldots & \boldsymbol{R}_c' \boldsymbol{a}_n \\ \boldsymbol{0}_{m\times2} & \boldsymbol{0}_{m\times2} & \ldots & \boldsymbol{0}_{m\times2} \\ l_1 \boldsymbol{q}_{n_1}^{\mathrm{T}} & \boldsymbol{0}_{n\times2} & \ldots & \boldsymbol{0}_{n\times2} \\ \boldsymbol{0}_{n\times2} & l_1 \boldsymbol{q}_{n_2}^{\mathrm{T}} & \ldots & \boldsymbol{0}_{n\times2} \\ \vdots & \vdots & \vdots & \vdots \\ \boldsymbol{0}_{n\times2} & \boldsymbol{0}_{n\times2} & \ldots & l_1 \boldsymbol{q}_{n_n}^{\mathrm{T}} \end{bmatrix} \tag{17}$$

Also, vector $\boldsymbol{u}$ in Eq. (7) is composed by thrust force vectors of quadrotors as the following equation:

$$\boldsymbol{u} = \begin{bmatrix} u_1 \boldsymbol{q}_{Q_1} \\ u_2 \boldsymbol{q}_{Q_2} \\ \vdots \\ u_n \boldsymbol{q}_{Q_n} \end{bmatrix} \tag{18}$$

in which u_i is net thrust force of the ith quadrotor while $\boldsymbol{q}_{Q_i}$ is unit vector of its direction.

3. Control design

In this section, proper control laws are designed so that quadrotors stabilize the container at a desired pose and suppress the fluid sloshing. Also, relative directions of the links with respect to the container should be stabilized at a desired attitude.

Tracking error of the container pose $\boldsymbol{e}$ is defined as

$$\boldsymbol{e} = \boldsymbol{p} - \boldsymbol{p}^{\mathrm{d}} \tag{19}$$

in which $\boldsymbol{p}^{\mathrm{d}}$ is desired pose of container.

Also, tracking errors for angles of the links are defined by

$$e_{\phi_i} = \phi_i - (\theta + \phi_i^{\mathrm{d}}) \tag{20}$$

in which e_{ϕ_i} represents ith link angle error.

In the recent equation, ϕ_i^{d} denotes desired relative angle of the ith link with respect to the lateral body fixed axis. Moreover, attitude tracking errors of the quadrotors are determined geometrically by

$$\begin{cases} \eta_i = 1 - \boldsymbol{q}_{Q_i}^{\mathrm{d}} \cdot \boldsymbol{q}_{Q_i} \\ e_i^{qQ} = \boldsymbol{q}_{Q_i}^{\mathrm{d}} \times \boldsymbol{q}_{Q_i} \\ e_{\Omega_i} = \dot{\phi}_{Q_i} - \dot{\phi}_{Q_i}^{\mathrm{d}} \end{cases} \tag{21}$$

in which the superscript d means desired.

3.1. Controller structure

Controller of the system is a hierarchical controller composed of container pose and sloshing controller, links' directions controller and quadrotors' attitude controllers. Container pose and sloshing controller together with links' directions controller determines thrust forces of the quadrotors and desired directions of the thrust forces of the quadrotors. On the other hand, quadrotors track the desired attitude by implementing their attitude controllers.

3.2. Quadrotor attitude tracking controller design

In this section, attitude controller of the quadrotor is proposed so that origin of the closed loop system of quadrotor attitude tracking error will be almost global exponential attractive.

Proposition 1. (*Stability of Quadrotor Attitude Controlled Flight Mode*). We consider rolling moment of each quadrotor which is defined as

$$\tau_i^{\mathrm{roll}} = J_{Q_i} \left(\ddot{\phi}_{Q_i}^{\mathrm{d}} - \frac{K_\Omega}{\varepsilon} e_{\Omega_i} - \frac{K_q}{\varepsilon^2} e_i^{qQ} \right) \tag{22}$$

for any positive constant K_Ω, K_q and $0 < \varepsilon < 1$. And we suppose that initial conditions satisfy the following inequalities:

$$\eta_i(0) < 2 \tag{23}$$

$$e_{\Omega_i}(0)^2 < \frac{2K_\mathrm{q}}{\varepsilon^2}(2 - \eta_i(0)) \tag{24}$$

Then, zero equilibrium points of tracking errors $(e_i^{q_\mathrm{Q}}, e_{\Omega_i}) = (0, 0)$ are exponentially stable. Furthermore, attitude tracking error η_i will converge to zero and desired attitude will be tracked by the quadrotor.

Proof. See Appendix A. □

Remark 3. Actually, Eqs. (23) and (24) define region of attraction for the origin of the closed loop system of attitude tracking error. Importance of the required initial conditions is described in Appendix A. One should note that these conditions are not too restrictive, because initial condition (23) only imposes that angle between desired direction of the thrust and its initial value should be less than 180°. Furthermore, region of attraction defined by Eq. (24) can be extended by increasing K_q or decreasing ε. Therefore, origin of closed loop system of attitude tracking error is almost global exponential attractive.

3.3. Controller design for container pose, sloshing and links' directions

To control pose of container, fluid sloshing and directions of the links, thrust force and desired attitude of each quadrotor are adopted as

$$u_i = \boldsymbol{\mu}_i . \boldsymbol{q}_{\mathrm{Q}_i}, \boldsymbol{q}_{\mathrm{Q}_i}^\mathrm{d} = \frac{\boldsymbol{\mu}_i}{\|\boldsymbol{\mu}_i\|} \tag{25}$$

where

$$\boldsymbol{\mu}_i = \boldsymbol{u}_{n_i}^\mathrm{d} \boldsymbol{q}_{n_i} + \boldsymbol{u}_{p_i}^\mathrm{d} \boldsymbol{q}_{p_i} \tag{26}$$

Also, desired parallel component of thrust force with the link denoted by $\boldsymbol{u}_{p_i}^\mathrm{d}$ in Eq. (26) is calculated from

$$\begin{cases} \boldsymbol{u}_p^\mathrm{d} = \boldsymbol{B}^\dagger(\boldsymbol{M}_p \boldsymbol{v} + \boldsymbol{F}_p) \\ \boldsymbol{u}_p^\mathrm{d} = [\boldsymbol{u}_{p_1}^\mathrm{d}, \boldsymbol{u}_{p_2}^\mathrm{d}, \ldots, \boldsymbol{u}_{p_n}^\mathrm{d}]^\mathrm{T} \end{cases} \tag{27}$$

where $\boldsymbol{B}^\dagger$ is Pseudo inverse of matrix $\boldsymbol{B}$ which is defined as

$$\boldsymbol{B} = \begin{bmatrix} \boldsymbol{q}_{p_1} & \boldsymbol{q}_{p_2} & \cdots & \boldsymbol{q}_{p_n} \\ -(\boldsymbol{R}_\mathrm{c}' \boldsymbol{a}_1)^\mathrm{T} \boldsymbol{q}_{p_1} & -(\boldsymbol{R}_\mathrm{c}' \boldsymbol{a}_2)^\mathrm{T} \boldsymbol{q}_{p_2} & \ldots & -(\boldsymbol{R}_\mathrm{c}' \boldsymbol{a}_n)^\mathrm{T} \boldsymbol{q}_{p_n} \end{bmatrix} \tag{28}$$

Remark 4. Pseudo inverse of matrix $\boldsymbol{B}$ exists if rank of matrix is three. Necessary condition for this is that number of quadrotors is more than or equal to three $n \geqslant 3$ .To ensure that matrix rank remains equal to three, it is sufficient that rank of matrix is initially 3 and relative directions of the links with respect to the container frame are stabilized at their initial orientation.

Remark 5. Maximum number of the quadrotors are not limited theoretically. However, systems with numerous quadrotors need high speed processors to calculate Pseudo inverse to determine $\boldsymbol{u}_p^\mathrm{d}$ in real time. Furthermore, maximum number of quadrotors is limited by the bandwidth of the communications.

In Eq. (27), matrix $\boldsymbol{M}_p$ and vector $\boldsymbol{F}_p$ are determined by

$$\begin{cases} \boldsymbol{M}_p = \boldsymbol{M}_{pp} - \boldsymbol{M}_{ps} \boldsymbol{M}_{ss}^{-1} \boldsymbol{M}_{sp} - \boldsymbol{M}_{pq} \boldsymbol{M}_{qq}^{-1} \boldsymbol{M}_{qp} \\ \boldsymbol{F}_p = \boldsymbol{f}_p - \boldsymbol{M}_{ps} \boldsymbol{M}_{ss}^{-1} \boldsymbol{f}_s - \boldsymbol{M}_{pq} \boldsymbol{M}_{qq}^{-1} \boldsymbol{f}_q \end{cases} \tag{29}$$

Furthermore, vector $\boldsymbol{v}$ in Eq. (27) is computed via

$$\boldsymbol{v} = -\boldsymbol{Y}^{-1}(\boldsymbol{H} + \boldsymbol{D}(\boldsymbol{\gamma})\dot{\boldsymbol{e}}) \tag{30}$$

in which γ_i are positive real constants and matrices $\boldsymbol{H}$ and $\boldsymbol{Y}$ are defined as

$$\begin{cases} \boldsymbol{Y} = \boldsymbol{D}(\boldsymbol{\lambda}) - \beta \boldsymbol{J}^\mathrm{T} \boldsymbol{J} \\ \boldsymbol{J} = [\,1 \cos\theta \quad 1\theta \sin\theta \quad \boldsymbol{h}\,] \\ \boldsymbol{H} = \beta\Big(-\dot{\boldsymbol{J}}^\mathrm{T} \dot{\boldsymbol{S}} + 2\boldsymbol{J}^\mathrm{T} \boldsymbol{D}(\boldsymbol{\omega}) \boldsymbol{D}(\boldsymbol{\xi}) \dot{\boldsymbol{S}} + \boldsymbol{J}^\mathrm{T} \boldsymbol{D}^2(\boldsymbol{\omega}) \boldsymbol{S} \\ -\boldsymbol{J}^\mathrm{T} \boldsymbol{S} \dot{\theta}^2 + \dot{\boldsymbol{S}}^\mathrm{T} \boldsymbol{S} \dot{\theta} \begin{bmatrix} 0 \\ 0 \\ 1 \end{bmatrix} \Big) + \boldsymbol{D}(\boldsymbol{\alpha}) \boldsymbol{e} \end{cases} \tag{31}$$

In the recent equation, $\omega_i = \sqrt{\dfrac{k_i}{m_i}}$ and $\xi_i = \dfrac{c_i}{2m_i\omega_i}$ denote the undamped natural frequencies and damping ratios of sloshing modes respectively, β denotes positive real constant gain of pose and sloshing controller, $\boldsymbol{\omega}$ and $\boldsymbol{\xi}$ denote vector composed of sloshing natural frequencies ω_i and damping ratios ξ_i respectively. Also, $\boldsymbol{\lambda}$ and $\boldsymbol{\alpha}$ in Eq. (31) are real positive constants. In addition, desired normal component of thrust of each quadrotor to its link denoted by $\boldsymbol{u}_{n_i}^\mathrm{d}$ in Eq. (26) is determined by the following definitions:

$$\begin{cases} \boldsymbol{u}_n^\mathrm{d} = \boldsymbol{L}^{-1} \boldsymbol{\Gamma} \\ \boldsymbol{\Gamma} = \boldsymbol{M}_{qp} \ddot{\boldsymbol{p}} + \boldsymbol{M}_{qq} \ddot{\boldsymbol{\phi}}^s + \boldsymbol{f}_q \\ \boldsymbol{L} = \boldsymbol{D}(\boldsymbol{l}) \end{cases} \tag{32}$$

where pose acceleration $\ddot{\boldsymbol{p}}$ can be measured by IMU sensors and $\ddot{\boldsymbol{\phi}}^s$ is defined as

$$\ddot{\boldsymbol{\phi}}^s = \boldsymbol{1}_{n \times 1} \ddot{\theta} + \ddot{\boldsymbol{\phi}}^\mathrm{d} - K_{\dot{\phi}} \dot{\boldsymbol{e}}_\phi - K_\phi \boldsymbol{e}_\phi \tag{33}$$

in which K_ϕ and $K_{\dot{\phi}}$ are positive real constants, $\boldsymbol{e}_\phi$ and $\dot{\boldsymbol{e}}_\phi$ are vector of errors of links' angles and first derivative of $\boldsymbol{e}_\phi$ with respect to time.

Proposition 2. (*Stability of container pose, liquid sloshing and links' directions tracking errors*). By adaption of magnitudes and desired directions for thrust forces as Eq. (25), ε^* can be found such that for all $\varepsilon < \varepsilon^*$, zero equilibrium point of tracking errors of links directions $(\boldsymbol{e}_\phi, \dot{\boldsymbol{e}}_\phi) = (0, 0)$ will be exponentially stable while $(\boldsymbol{e}, \dot{\boldsymbol{e}}, \boldsymbol{S}, \dot{\boldsymbol{S}}) = (0, 0, 0, 0)$ will be an asymptotically stable equilibrium point for closed loop system of tracking errors of container pose and sloshing modes.

Proof. See Appendix B. □

4. Simulation

In this section, designed feedback control laws are examined in stabilizing a container by three identical quadrotors considering only two modes of sloshing. To verify the performance of the proposed control laws, initial conditions and physical properties of container and sloshing liquid are adopted from Ref.[10] as

$$\begin{cases} h_0 = -0.008\ \text{m}, h_1 = 0.042\ \text{m}, h_2 = 0.113\ \text{m} \\ k_1 = 258\ \text{N/m}, k_2 = 22.5\ \text{N/m} \\ c_1 = 0.038\ \text{N}\cdot\text{s/m}, c_2 = 0.002\ \text{N}\cdot\text{s/m} \\ m_0 = 7.95\ \text{kg}, m_1 = 1.43\ \text{kg}, m_2 = 0.04\ \text{kg}, m_c = 1.5\ \text{kg} \\ I_0 = 0.042\ \text{kg.m}^2, I_c = 0.011\ \text{kg.m}^2 \\ \boldsymbol{r}_c(0) = \begin{bmatrix} 1 \\ 1 \end{bmatrix}, \theta(0) = \frac{\pi}{4}, s_1(0) = 0.03, s_2(0) = -0.01 \\ \dot{\boldsymbol{r}}_c(0) = \begin{bmatrix} 0 \\ 0 \end{bmatrix}, \dot{\theta}(0) = \dot{s}_1(0) = \dot{s}_2(0) = 0 \end{cases} \tag{34}$$

Values of the control parameters $\boldsymbol{\alpha}, \boldsymbol{\lambda}, \beta$ and $\boldsymbol{\gamma}$ are the same as values selected in Ref.[10] for them:

$$\begin{cases} \boldsymbol{\alpha} = [15, 15, 15] \\ \boldsymbol{\lambda} = [6, 6, 6] \\ \beta = 1 \\ \boldsymbol{\gamma} = [30, 50, 30] \end{cases} \tag{35}$$

Same as the problem defined in this reference, quadrotors should stabilize container at $\boldsymbol{r}_c^d = \begin{bmatrix} 0 \\ 0 \end{bmatrix}, \theta^d = 0$ while suppressing sloshing modes simultaneously. Also, quadrotors should control rigid links' direction relative to container so that rank of matrix $\boldsymbol{B}$ will be equal to 3 all the time. To do this, if initial conditions of rigid links' direction are proper then quadrotors should try to keep these directions fixed relative to the container during the transport. Lengths of the links are 2 meters and initially their angles are set arbitrarily as

$$\begin{cases} \phi_1(0) = 3\pi/4, \dot{\phi}_1(0) = 0 \\ \phi_2(0) = 11\pi/12, \dot{\phi}_2(0) = 0 \\ \phi_3(0) = 3\pi/4, \dot{\phi}_3(0) = 0 \end{cases} \tag{36}$$

In other words, links 1 and 3 are perpendicular to container edge while angle between link 2 and lateral axis of container fixed frame is $\frac{2\pi}{3}$. Controllers will try to keep these relative orientations constant. Moreover, positions of attachment points of the links in the container fixed frame are

$$\begin{cases} \boldsymbol{a}_1 = a\hat{\boldsymbol{j}} + b\hat{\boldsymbol{k}} \\ \boldsymbol{a}_2 = -a\hat{\boldsymbol{j}} + b\hat{\boldsymbol{k}} \\ \boldsymbol{a}_3 = b\hat{\boldsymbol{k}} \end{cases} \tag{37}$$

where $a = 1$ m is radius of the container and $b = 2$ m is height of the container edge from its center of mass. Physical properties of the quadrotors are imported from Ref.[43] to the simulation as

$$\begin{cases} m_{Q_i} = 0.65\ \text{kg} \\ J_{Q_i} = 7.5 \times 10^{-3}\ \text{kg}\cdot\text{m}^2 \end{cases} \tag{38}$$

Considering conditions introduced by Eqs. (23) and (24), initial conditions for directions of thrust vectors of the quadrotors are set as

$$\begin{cases} \boldsymbol{q}_{Q_1}(0) = \boldsymbol{q}_{Q_2}(0) = \boldsymbol{q}_{Q_3} = \begin{bmatrix} 0 \\ 1 \end{bmatrix} \\ \dot{\phi}_{Q_1}(0) = \dot{\phi}_{Q_2}(0) = \dot{\phi}_{Q3}(0) = 0 \end{cases} \tag{39}$$

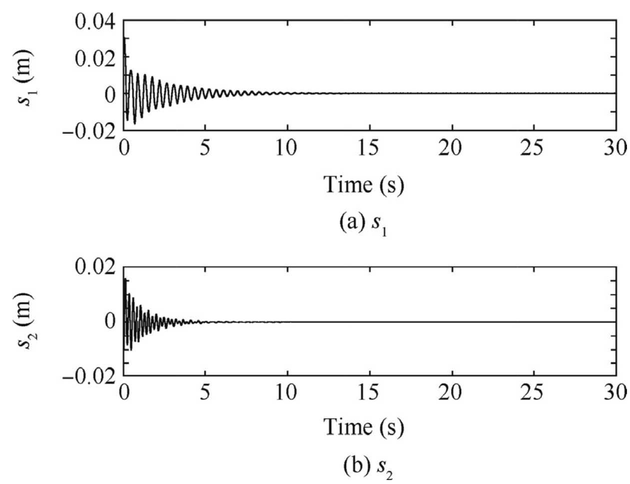

Fig. 4 Time response of s_1 and s_2.

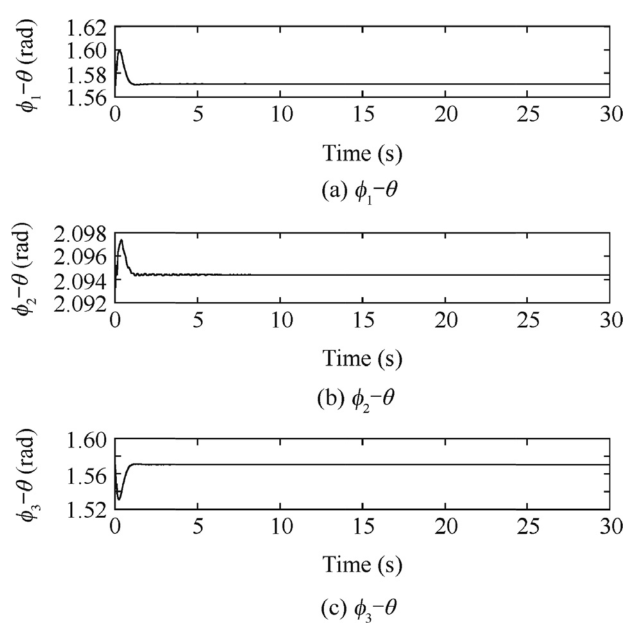

Fig. 5 Time response of links' directions relative to container.

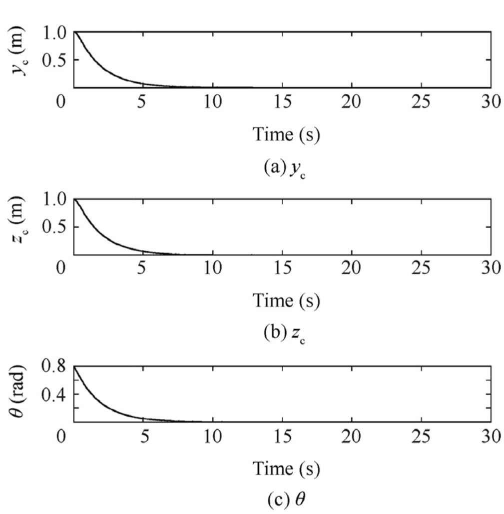

Fig. 3 Time response of container pose.

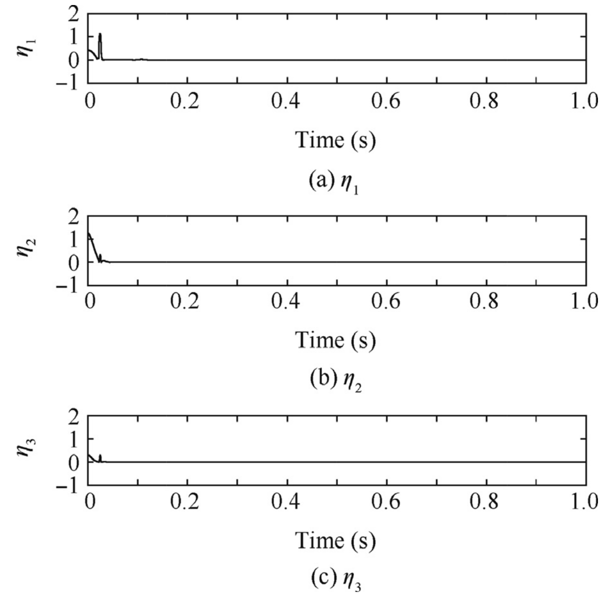

Fig. 6 Time response of attitude error functions of quadrotors $\eta_i, i = 1, 2, 3$.

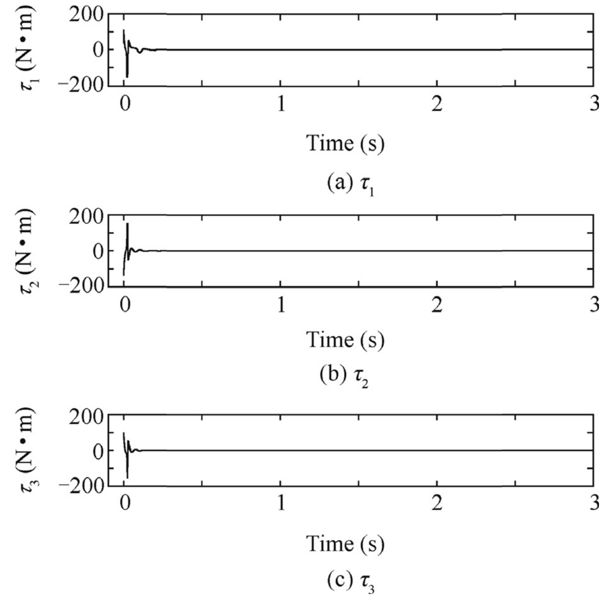

Fig. 8 Rolling torques of quadrotors.

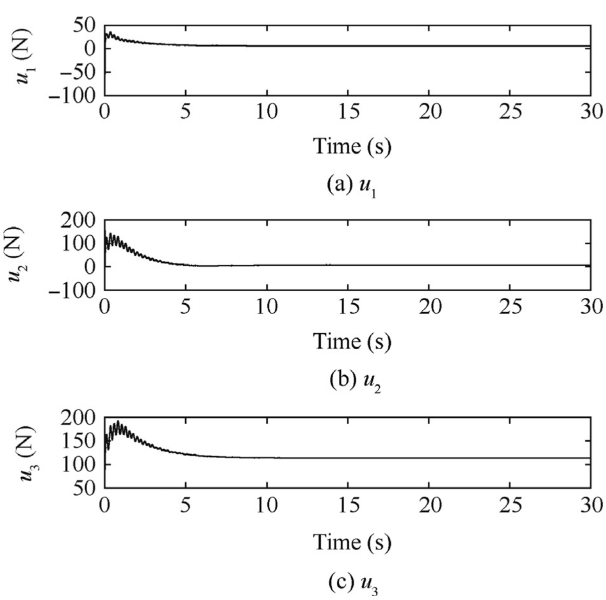

Fig. 7 Thrust forces of quadrotors.

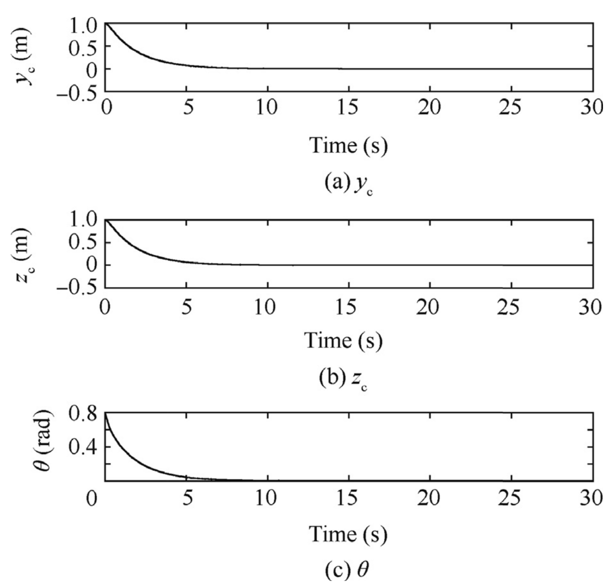

Fig. 9 Time response of container pose by controller proposed in Ref.[36]

Control parameters for the links' directions and quadrotor attitudes are chosen as

$$\begin{cases} K_\phi = 25 \\ K_{\dot{\phi}} = 8 \\ K_{\mathrm{q}} = 180 \\ K_\Omega = 20 \\ \varepsilon = 0.1 \end{cases} \tag{40}$$

Time responses of the states of the system (7) where the proposed feedback control laws are implemented are demonstrated in Figs. 3–6. It can be seen in these figures that the container is stabilized at origin horizontally successfully (Fig. 3). Moreover, sloshing modes are suppressed and stabilized well too (Fig. 4). Links' directions are stabilized at their initially established directions approximately during the mission (Fig. 5). In Fig. 6, attitude error functions of the quadrotors η_i are depicted. Due to implemented command filters to calculate $\dot{\phi}^{\mathrm{d}}_{\mathrm{Q}_i}$ and $\ddot{\phi}^{\mathrm{d}}_{\mathrm{Q}_i}$, some peaks occur in value of η_i. However, attitude error functions of quadrotors η_i have been stabilized at zero quickly. Control inputs (thrust forces and rolling torques of quadrotors) are depicted in Figs. 7 and 8. Feasibility of this mission for selected quadrotors has not been studied here.

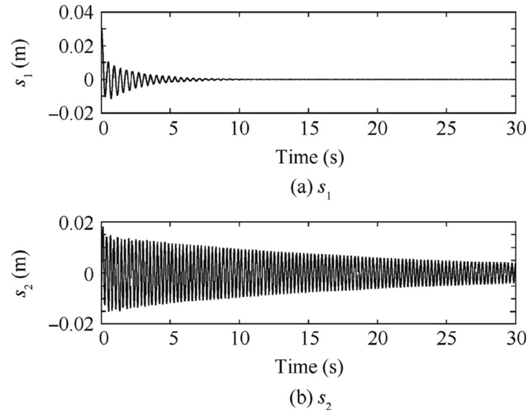

Fig. 10 Time response of s_1 and s_2 pose by controller proposed in Ref.[36]

To compare capabilities of the proposed control law with the existing slung load transport controllers in the literature, the load stabilization mission is simulated by the controller proposed in Ref.[36], As depicted in Figs. 9 and 10, although attitude and position of the container are stabilized by the controller, liquid sloshing is not controlled at all. In the other words, the proposed controller in the present study can control the load position, attitude and fluid sloshing simultaneously while the controller proposed in Ref.[36] controls only the position and attitude of the load.

5. Conclusions

In this study, aerial transport problem of a liquid filled container suspended via rigid massless links from quadrotors has been investigated. Feedback control laws have been introduced so that quadrotors can stabilize container at the desired pose and eliminate liquid sloshing. Also, feedback control laws enable quadrotor to control links' directions relative to the tank. Stability of zero point for closed loop system of tracking errors has been established by Lyapunov stability theorem along with an argument about singularly perturbed systems. Moreover, effectiveness of the designed control laws has been examined in simulation. Moreover, superiority of the proposed control laws over an existing slung load controller is demonstrated in simulations. Experimental verification of the proposed control laws may be challenging due to measurements of sloshing states needed for feedback, which can be solved by designing a proper observer. Also, designing controllers which are robust against parametric uncertainties and disturbances may be included in future works.

Appendix A

Proof of Proposition 1. After defining $k_q = \dfrac{K_q}{\varepsilon^2}, k_\Omega = \dfrac{K_\Omega}{\varepsilon}$, attitude tracking error dynamics of each quadrotor can be described by Eq. (22) as

$$\dot{e}_{\Omega_i} = -k_q e_i^{q_Q} - k_\Omega e_{\Omega_i} \tag{A1}$$

Therefore, a Lyapunov function is introduced as

$$V_{\eta_i} = k_q \eta_i + \frac{1}{2}\|e_{\Omega_i}\|^2 \tag{A2}$$

By considering that $\dot{\eta}_i = e_i^{q_Q} \cdot e_{\Omega_i}$, derivative of the Lyapunov function with respect to the time can be found as

$$\dot{V}_{\eta_i} = -k_{\Omega_i}\|e_{\Omega_i}\|^2 \tag{A3}$$

Consequently, $e_{\Omega_i} \to 0$ and $V_{\eta_i}(t) \leqslant V_{\eta_i}(0)$. Using Eq. (A1), it can be concluded that $e_i^{q_Q} \to 0$. So, one can conclude that $\eta_i \to 0$ or $\eta_i \to 2$. According to $V_{\eta_i}(t) \leqslant V_{\eta_i}(0)$, one can obtain that $\eta_i(t) \leqslant \dfrac{V_{\eta_i}(0)}{k_q}$. Using conditions defined by Eqs. (23) and (24), it can be found that $\eta_i(t) \leqslant \dfrac{V_{\eta_i}(0)}{k_q} < 2$. Therefore, attitude tracking error η_i will not tend to 2. Consequently, desired attitude of the quadrotor will be tracked because $\eta_i \to 0$. This proof is a detailed version of the proof introduced in lemma 11.23 of Ref.[44] □

Appendix B

Proof of Proposition 2. Define $\bar{e}_i^{q_Q} = \dfrac{e_i^{q_Q}}{\varepsilon}$, and dynamics of tracking errors of quadrotor attitudes can be rewritten as

$$\begin{aligned} &\varepsilon \dot{\bar{e}}_i^{q_Q} = e_{\Omega_i}(q_{Q_i}.q_{Q_i}^{\mathrm{d}}) \\ &\varepsilon \dot{e}_{\Omega_i} = -K_{\Omega_i} e_{\Omega_i} - K_q \bar{e}_i^{q_Q} \end{aligned} \tag{B1}$$

Set $\varepsilon = 0$, and then one will have $\boldsymbol{q}_{Q_i} \equiv \boldsymbol{q}_{Q_i}^{\mathrm{d}}$ and so $\boldsymbol{u}_p \equiv \boldsymbol{u}_p^{\mathrm{d}}$ and $\boldsymbol{u}_n \equiv \boldsymbol{u}_n^{\mathrm{d}}$. Therefore, dynamics of direction errors of the links in slow model of system will be

$$\ddot{\boldsymbol{e}}_\phi = -K_{\dot{\phi}}\dot{\boldsymbol{e}}_\phi - K_\phi \boldsymbol{e}_\phi \tag{B2}$$

Consequently, point $(\boldsymbol{e}_\phi, \dot{\boldsymbol{e}}_\phi) = (0, 0)$ is an exponentially stable equilibrium point for the closed loop system presented by Eq. (B2).

According to the equations of motion of system, one can find that

$$\begin{aligned} &\ddot{\boldsymbol{S}} = -\boldsymbol{M}_{ss}^{-1}(\boldsymbol{M}_{sp}\ddot{\boldsymbol{p}} + \boldsymbol{f}_s) \\ &\ddot{\boldsymbol{\phi}} = -\boldsymbol{M}_{qq}^{-1}(\boldsymbol{M}_{qp}\ddot{\boldsymbol{p}} + \boldsymbol{f}_q - \boldsymbol{B}_q\boldsymbol{u}) \end{aligned} \tag{B3}$$

Then, dynamics of the container pose can be presented by

$$\boldsymbol{M}_p\ddot{\boldsymbol{p}} + \boldsymbol{F}_p = \boldsymbol{B}\boldsymbol{u}_p \tag{B4}$$

Definition of $\boldsymbol{M}_p, \boldsymbol{F}_p$ and $\boldsymbol{B}$ can be found from Eqs. (29) and (28) respectively. As described formerly, in the slow model $\boldsymbol{u}_p \equiv \boldsymbol{u}_p^{\mathrm{d}}$ and so from Eq. (27), it can be concluded that

$$\begin{aligned} &\ddot{\boldsymbol{e}} = \boldsymbol{v} \\ &\ddot{\boldsymbol{S}} = -\boldsymbol{J}\boldsymbol{v} + \boldsymbol{R}, \boldsymbol{R} = -2\boldsymbol{D}(\boldsymbol{\xi})\boldsymbol{D}(\boldsymbol{\omega})\dot{\boldsymbol{S}} - (\boldsymbol{D}^2(\boldsymbol{\omega}) - \dot{\theta}^2)\boldsymbol{S} \end{aligned} \tag{B5}$$

A Lyapunov function V can be candidate as

$$V = \frac{1}{2}[\boldsymbol{e}^{\mathrm{T}}\boldsymbol{D}(\boldsymbol{\alpha})\boldsymbol{e} + \dot{\boldsymbol{e}}^{\mathrm{T}}\boldsymbol{D}(\boldsymbol{\lambda})\dot{\boldsymbol{e}} + \beta(\dot{\boldsymbol{S}}^{\mathrm{T}}\dot{\boldsymbol{S}} + \boldsymbol{S}^{T}\boldsymbol{D}^2(\boldsymbol{\omega})\boldsymbol{S} - 2\dot{\boldsymbol{S}}^{\mathrm{T}}\boldsymbol{J}\dot{\boldsymbol{e}})] \tag{B6}$$

in which it is assumed that

$$\dot{\boldsymbol{e}}^{\mathrm{T}}\boldsymbol{D}(\boldsymbol{\lambda})\dot{\boldsymbol{e}} + \beta(\dot{\boldsymbol{S}}^{\mathrm{T}}\dot{\boldsymbol{S}} - 2\dot{\boldsymbol{S}}^{\mathrm{T}}\boldsymbol{J}\dot{\boldsymbol{e}}) > 0 \tag{B7}$$

Then, V will be positive definite. For example, consider two modes of sloshing and $\lambda_1 = \lambda_2 = \lambda_3 = \lambda$, and then sufficient conditions for satisfying Eq. (B7) are

$$\begin{cases} \lambda > \beta(1 + h_1^2) \\ -\beta(2\lambda - \beta(h_1 - h_2)^2) + \lambda(\lambda - \beta(h_1^2 + h_2^2)) > 0 \end{cases} \tag{B8}$$

Time derivative of V using the equations of motion for the slow system and the feedback control law will be

$$\dot{V} = \dot{\boldsymbol{e}}^{\mathrm{T}}(\boldsymbol{Y}\boldsymbol{v} + \boldsymbol{H}) - \dot{\boldsymbol{S}}^{\mathrm{T}}\boldsymbol{D}(\xi)\boldsymbol{D}(\boldsymbol{\omega})\dot{\boldsymbol{S}} \tag{B9}$$

Now if $\boldsymbol{v}$ is adopted as Eq. (30), then

$$\dot{V} = -\dot{\boldsymbol{e}}^{\mathrm{T}}\boldsymbol{D}(\gamma)\dot{\boldsymbol{e}} - \dot{\boldsymbol{S}}^{\mathrm{T}}\boldsymbol{D}(\xi)\boldsymbol{D}(\boldsymbol{\omega})\dot{\boldsymbol{S}} \tag{B10}$$

which satisfies $\dot{V} \leqslant 0$. Using LaSalle's principle,[45] it is easy to prove asymptotic stability of the origin of the closed loop system defined by Eq. (B5) and the proposed feedback control law (30). Using theorem 11.2 of Ref.[45], there exist ε^* such that for all $0 < \varepsilon < \varepsilon^*$, differences between states of full model and slow model are all in order of $O(\varepsilon)$ uniformly. $\square$

References

1. Carton P, Chrétien JP, Maurette M. Simulation and control of space manipulators bearing complex payloads. *IFAC ProcVolumes* 1989;**22**(7):127–32.
2. Feddema JT, Dohrmann CR, Parker GG, Robinett RD, Romero DJ, Schmitt DJ. Control for slosh-free motion of an open container. *IEEE Cont Syst* 1997;**17**(1):29–36.
3. Xing GQ, Bainum PM, Li F. Design of a reduced order H∞ robust controller for an expendable launch vehicle in the presence of structured and unstructured parameter uncertainty1. *Acta Astronaut* 1997;**41**(2):121–30.
4. Yano K, Terashima K. Robust liquid container transfer control for complete sloshing suppression. *IEEE Trans Cont Syst Technol* 2001;**9**(3):483–93.
5. Yano Ki, Higashikawa S, Terashima K. Motion control of liquid container considering an inclined transfer path. *Cont Eng Pract* 2002;**10**(4):465–72.
6. Yano K, Terashima K. Sloshing suppression control of liquid transfer systems considering a 3-D transfer path. *IEEE/ASME Trans Mechatron* 2005;**10**(1):8–16.
7. Bandyopadhyay B, Gandhi PS, Kurode S. Sliding mode observer based sliding mode controller for slosh-free motion through PID scheme. *IEEE Trans Ind Electron* 2009;**56**(9):3432–42.
8. Kurode S, Spurgeon SK, Bandyopadhyay B, Gandhi PS. Sliding mode control for slosh-free motion using a nonlinear sliding surface. *IEEE/ASME Trans Mechatron* 2013;**18**(2):714–24.
9. Reyhanoglu M, Rubio HJ. Nonlinear dynamics and control of space vehicles with multiple fuel slosh modes. *Cont Eng Pract* 2012;**20**(9):912–8.
10. Reyhanoglu M, Rubio HJ. Nonlinear modeling and control of slosh in liquid container transfer via a PPR robot. *Commun Nonlinear Sci Numer Simul* 2013;**18**(6):1481–90.
11. Rubio HJ, Reyhanoglu M. Thrust-vector control of a three-axis stabilized upper-stage rocket with fuel slosh dynamics. *Acta Astronaut* 2014;**98**:120–7.
12. Zang Q, Huang J, Liang Z. Slosh suppression for infinite modes in a moving liquid container. *IEEE/ASME Trans Mechatron* 2015;**20**(1):217–25.
13. Lindsey Q, Mellinger D, Kumar V. Construction with quadrotor teams. *Auton Robot* 2012;**33**(3):323–36.
14. Dai S, Lee T, Bernstein DS. Adaptive control of a quadrotor UAV transporting a cable-suspended load with unknown mass. *53rd IEEE Conference on Decision and Control*; 2014 Dec 15–17; Los Angeles, USA. Piscataway: IEEE Press; 2015. p. 6149–54.
15. Faust A, Palunko I, Cruz P, Fierro R, Tapia L. Automated aerial suspended cargo delivery through reinforcement learning. *Artif Intell* 2014;**247**:381–98.
16. Cruz P, Fierro R. Autonomous lift of a cable-suspended load by an unmanned aerial robot. *2014 IEEE Conference on Control Applications (CCA)*; 2014 Oct 8–10; Juan Les Antibes, France. Piscataway: IEEE Press; 2014. p. 802–7.
17. Fusato D, Guglieri G, Celi R. Flight dynamics of an articulated rotor helicopter with an external slung load. *J Am Helicopter Soc* 2001;**46**(1):3–13.
18. Sreenath K, Lee T, Kumar V. Geometric control and differential flatness of a quadrotor UAV with a cablesuspended load. *52nd IEEE Conference on Decision and Control*; 2013 Oct 10–13; Firenze, Italy; Piscataway: IEEE Press; 2013. p. 2269–74.
19. Goodarzi FA, Lee D, Lee T. Geometric control of a quadrotor UAV transporting a payload connected via flexible cable. *Int J Cont Autom Syst* 2015;**13**(6):1486–98.
20. Goodarzi FA, Lee D, Lee T. Geometric stabilization of a quadrotor UAV with a payload connected by flexible cable. *2014 American Control Conference*; 2014 June 4–6; Portland, USA; Piscataway: IEEE Press; 2014. p. 4925–30.
21. Faust A, Palunko I, Cruz P, Fierro R, Tapia L. Learning swing-free trajectories for UAVs with a suspended load. *2013 IEEE International Conference on Robotics and Automation*; 2013 May 6–10; Karlsruhe, Germany; Piscataway: IEEE Press; 2013. p. 4902–9.
22. Tang S, Kumar V. Mixed integer quadratic program trajectory generation for a quadrotor with a cable-suspended payload. *2015 IEEE International Conference on Robotics and Automation (ICRA)*; 2015 May 26–30; Seattle, USA; Piscataway: IEEE Press; 2013. p. 2216–22.
23. Oktay T, Sultan C. Modeling and control of a helicopter slung-load system. *Aerosp Sci Technol* 2013;**29**(1):206–22.
24. Feng Y, Rabbath CA, Su CY. Modeling of a micro UAV with slung payload. In: Valavanis KP, Vachtsevanos GJ, editors. *Handbook of unmanned aerial vehicles*. Dordrecht: Springer, Netherlands; 2015. p. 1257–72.
25. Notter S, Heckmann A, McFadyen A, Gonzalez F. Modelling, simulation and flight test of a model predictive controlled multirotor with heavy slung load. *IFAC-PapersOnLine* 2016;**49**(17):182–7.
26. Potter JJ, Adams CJ, Singhose W. A planar experimental remote-controlled helicopter with a suspended load. *IEEE/ASME Trans Mechatron* 2015;**20**(5):2496–503.
27. Palunko I, Faust A, Cruz P, Tapia L, Fierro R. A reinforcement learning approach towards autonomous suspended load manipulation using aerial robots. *2013 IEEE International Conference on Robotics and Automation*; 2013 May 6–10; Karlsruhe, Germany; Piscataway: IEEE Press; 2013. p. 4896–901.
28. Pounds PEI, Bersak DR, Dollar AM. Stability of small-scale UAV helicopters and quadrotors with added payload mass under PID control. *Auton Robot* 2012;**33**(1):129–42.
29. Sreenath K, Michael N, Kumar V. Trajectory generation and control of a quadrotor with a cable-suspended load - A differentially-flat hybrid system. *2013 IEEE International Conference on Robotics and Automation*; 2013 May 6–10; Karlsruhe, Germany; Piscataway: IEEE Press; 2013. p. 4888–95.
30. Palunko I, Fierro R, Cruz P. Trajectory generation for swing-free maneuvers of a quadrotor with suspended payload: A dynamic programming approach. *2012 IEEE International Conference on Robotics and Automation*; 2012 May 14–18; Saint Paul, USA; Piscataway: IEEE Press; 2012. p. 2691–7.

31. Bisgaard M, la Cour-Harbo A, Johnson EN, Bendtsen JD. Vision aided state estimator for helicopter slung load system. *IFAC Proc* 2007;**40**(7):425–30.
32. Mellinger D, Shomin M, Michael N, Kumar V. Cooperative grasping and transport using multiple quadrotors. In: Martinoli A, Mondada F, Correll N, Mermoud G, Egerstedt M, Hsieh MA, et al., editors. *Distributed autonomous robotic systems: The 10th international symposium*. Heidelberg: Springer, Berlin Heidelberg; 2013. p. 545–58.
33. Kumar V, Sreenath K. Dynamics, control and planning for cooperative manipulation of payloads suspended by cables from multiple quadrotor robots. *Robot: Sci Syst* 2013;1–8.
34. Lee T, Sreenath K, Kumar V. Geometric control of cooperating multiple quadrotor UAVs with a suspended payload. *52nd IEEE Conference on Decision and Control*; 2013 Oct 10–13; Firenze, Italy; Piscataway: IEEE Press; 2013. p. 5510–5.
35. Lee T. Geometric control of multiple quadrotor UAVs transporting a cable-suspended rigid body. *53rd IEEE Conference on Decision and Control*; 2014 Dec 15–17; Los Angeles, USA; Piscataway: IEEE Press; 2015. p. 6155–60.
36. Wu G, Sreenath K. Geometric control of multiple quadrotors transporting a rigid-body load. *53rd IEEE Conference on Decision and Control*; 2014 Dec 15–17; Los Angeles, USA; Piscataway: IEEE Press; 2015. p. 6141–8.
37. Parra-Vega V, Sanchez A, Izaguirre C, Garcia O, Ruiz-Sanchez F. Toward aerial grasping and manipulation with multiple UAVs. *J Intell Robot Syst* 2013;**70**(1):575–93.
38. He W, Ge SS. Cooperative control of a nonuniform gantry crane with constrained tension. *Autom* 2016;**66**:146–54.
39. He W, Chen Y, Yin Z. Adaptive neural network control of an uncertain robot with full-state constraints. *IEEE Trans Cybern* 2016;**46**(3):620–9.
40. He W, Dong Y, Sun C. Adaptive neural impedance control of a robotic manipulator with input saturation. *IEEE Trans Syst Man Cybern: Syst* 2016;**46**(3):334–44.
41. He W, Ouyang Y, Hong J. Vibration control of a flexible robotic manipulator in the presence of input deadzone. *IEEE Trans Ind Inform* 2017;**13**(1):48–59.
42. Dai L, Xu L, Setiawan B. A new non-linear approach to analysing the dynamic behaviour of tank vehicles subjected to liquid sloshing. *Mech Eng, Part K; J Multi-body Dyn* 2005;**219**(1):75–86.
43. Bouabdallah S. Design and control of quadrotors with application to autonomous flying [dissertion]. Lausanne: EPFL University; 2007.
44. Bullo F, Lewis AD. *Geometric control of mechanical systems*. New York-Heidelberg-Berlin: Springer-Verlag; 2004.
45. Khalil HK. *Nonlinear systems*. New Jersey: Prentice Hall; 2002.